Radar Observations of Changing Orientations of Hydrometeors in Thunderstorms

JAMES I. METCALF

Atmospheric Sciences Division, Phillips Laboratory, Hanscom Air Force Base, Massachusetts

(Manuscript received 19 February 1994, in final form 27 July 1994)

ABSTRACT

Changing orientations of hydrometeors due to rapidly changing electric fields in thunderstorms were observed by the 11-cm polarimetric Doppler radar that was operated by the Geophysics Directorate of Phillips Laboratory in Sudbury, Massachusetts. The radar transmitted signals of right circular polarization and received signals of right and left circular polarization in a dual-channel receiver. The effects of electric fields at heights of 7–11 km in thunderstorms appear as differential phase shifts in the propagation medium due to highly oriented ice particles. These effects are evident in rangewise profiles of the cross-covariance amplitude ratio derived from the two received signals. Some of the observations show specific differential phase shifts up to 1.6° km^{-1} in range intervals of a few kilometers and up to 0.8° km^{-1} in range intervals up to 18 km with a distinct tendency of increasing phase shift prior to an occurrence of lightning. Many occurrences of lightning were accompanied by sudden increases or decreases of the phase shift, indicative of corresponding changes in the magnitude of the electric field, or by sudden changes in the orientation of the cross-covariance amplitude ratio, indicative of sudden changes of the canting angle of the propagation medium. Following such a sudden change, the propagation medium usually returned to its prior state in a time interval between several seconds and several tens of seconds, depending on the electrical activity of the storm. These results support the possibility of characterizing the electric field in clouds by radar measurements.

1. Introduction

It has long been known that electric fields affect the orientations of hydrometeors in thunderstorms. These effects have been observed in the past by radars with wavelengths of 1.8 cm (Hendry and McCormick 1976; Hendry and Antar 1982) and 3.1 cm (Krehbiel et al. 1991, 1992, 1994). During 1991 and 1992 these effects were observed by the 11-cm polarimetric Doppler radar (Metcalf et al. 1993) that was operated in Sudbury, Massachusetts, by the Geophysics Directorate of Phillips Laboratory (formerly the Air Force Geophysics Laboratory). The principal purposes of these observations were to identify and measure quantities that could be related to the electric field in thunderstorms and to investigate the temporal and spatial structure of the field as revealed by these quantities. Because of the advantages of radar wavelengths of 10–11 cm for weather surveillance in general, it is of particular interest to assess the utility of these wavelengths for observing phenomena related to the electric field. The specification of an optimum radar wavelength for detecting the effects of electric fields in thunderstorms is beyond the scope of the present investigation.

In the following sections we describe the radar and our procedures for data acquisition and analysis. We discuss in detail observations from 3 days during 1992, summarize other observations during 1991 and 1992, and conclude with a discussion of the relationships between the observed phenomena and cloud microphysical characteristics.

Corresponding author address: James Metcalf, Phillips Laboratory/GPAA, 29 Randolph Rd., Hanscom AFB, MA 01731-3010.

2. The radar

The radar operates with a wavelength of 11.1 cm (carrier frequency of 2.71 GHz) and transmits pulses of 1-μs duration and peak power up to 1 MW. For the observations described below, we used a peak power of 850 kW and a pulse repetition time of 1.03 ms (pulse repetition frequency of 971 Hz), which yields an unambiguous range of 154.5 km and unambiguous Doppler velocity of ± 26.87 m s^{-1}. The minimum detectable reflectivity was 1 dBZ at 75-km range.

The radar is capable of operating in a full-matrix mode, in which it transmits successive pulses with alternating polarization (either horizontal and vertical or right and left circular) and receives signals with polarizations identical and orthogonal to that of the transmitted signal. For the observations described below we operated in a half-matrix mode. The radar transmitted signals of right circular polarization and coherently received signals of right and left circular polarization, respectively, denoted by E_1 and E_2, of which E_2 is the larger or "main" signal. In the full-matrix or half-matrix mode, the receiver output comprises the logarithmic power and the in-phase and

quadrature components of the amplitude of each received polarization. These six quantities were sampled in 50 selectable range gates, digitized, and recorded as continuous time series for off-line analysis. The data acquisition control program allowed a user to select the range to the first gate and the range increment between gates as 150, 300, 600, 1200, or 2400 m.

3. Procedures

From January 1991, when we completed the installation of a new polarimetric data acquisition system, through September 1992 we observed most of the significant precipitation events within our surveillance area with particular emphasis on convective storms. In preparation for polarimetric observations related to electric fields, we used the radar in a surveillance mode to observe developing storms while we monitored the locations of cloud-to-ground lightning to assess the electrical activity of storms. Lightning locations recorded by Geomet Data Services, Inc. [formerly by the State University of New York at Albany (Orville et al. 1983)] were received and archived by the Geophysics Directorate at Hanscom Air Force Base and displayed in nearly real time at the radar field site. We use the lightning data mainly as indicators of storm electrical activity; because the probability of detection by the network is estimated to be about 70%, we do not attempt to relate specific phenomena observed by radar to specific strikes recorded by the network.

We repeatedly estimated the region of greatest electrical activity in a storm; set the azimuth, elevation angles, and range gates to observe that region at an altitude of several kilometers; and recorded polarimetric data for an interval of several minutes. After several minutes of observation, we either attempted to follow the center of electrical activity by turning the antenna a few degrees in azimuth or returned to a surveillance mode to establish new parameters for a subsequent observation. We made all our observations at a fixed azimuth angle and either at a fixed elevation angle or within a small sector of elevation angle. We monitored the logarithmic power from both receiver channels on an oscilloscope, that is, an "A-scope" display, to observe echoes from lightning channels that intersected the radar beam. Lightning echoes are identifiable as brief, relatively coherent enhancements of the received signals. Their duration is typically a few tenths of a second. Other characteristics of these echoes were discussed by Metcalf (1988) and by Williams et al. (1989). We use the occurrence of lightning echoes as a time reference for changes of the electric field and, thus, as a guide for analysis and interpretation of the radar data. Although we had real-time displays of reflectivity and Doppler mean velocity, our data acquisition was seriously impeded by the lack of a real-time display of polarimetric quantities.

We analyze the data recorded at constant azimuth and elevation angles by examining segments typically several seconds in length near the times when we observed lightning echoes. We analyze the elevation scans by comparing sequential scans in a series. The key polarimetric quantities we examine are the circular depolarization ratio (CDR), which is the ratio of power received in the transmission channel to power received in the orthogonal ("main") channel, and quantities derived from the cross-covariance of the two received signals. We have found that the effects of changing electric fields on the orientations of hydrometeors appear mainly in quantities related to polarization differential propagation characteristics, rather than in quantities directly related to backscatter. As we analyze the data, we first examine individual scans to discern the presence of propagation effects and then compare sequential scans to identify significant changes of these effects. Finally, we relate the changing propagation effects to the electrical activity of the storm. In particular, we attempt to relate the changes of propagation effects to the occurrence of lightning.

During the spring and summer of 1991 we acquired polarimetric data on 9 days when lightning occurred within our surveillance area. These observations, most of which were made at fixed azimuth and elevation angles, provided only occasional evidence of changing orientations of hydrometeors coincident with lightning (Metcalf 1992). In over 4 h of polarimetric data, we recorded 183 echoes from lightning channels that intersected the radar beam. Only about 10% of these events were accompanied by significant changes of polarimetric quantities, that is, changes of more than 1 dB in the CDR, 5% in the cross correlation, or 10° in the phase of the cross-covariance in several range gates. None of these observations revealed cyclical changes of the polarimetric quantities such as have been observed elsewhere and associated with cyclical changes of the electric field.

In 1992 we sought to document the spatial structure of the orientation phenomena by repeatedly scanning small sectors of the elevation angle, following a suggestion by Dr. Paul Krehbiel. There were more thunderstorm days in 1992 than in 1991, and although we missed a few of them due to equipment malfunctions, we recorded nearly 6 h of polarimetric data during observations of thunderstorms on 10 days. These observations are summarized in Table 1. We recorded nearly 900 lightning echoes, including more than 100 on each of 4 days. Observations from 3 of these days are discussed in detail in section 5.

4. Theory

McCormick and Hendry (1975) showed that quantities derived from the cross-covariance of the two circularly polarized received signals are of particular importance for observation of the orientations of hydrometeors. In the absence of propagation effects, for example, the cross correlation of the two received sig-

TABLE 1. Polarimetric observations of thunderstorms during 1992.

Date	Duration of operation (EST)	Number of polarimetric observations	Total duration of polarimetric data (min)	Number of lightning echoes
8 June	1320–1730	7	33	146
20 June	1200–1830	9	56	83
24 June	0730–2200	4	25	46
9 July	1440–1610	2	6	4
14 July	1800–2100	6	22	136
17–18 July	2200–0330	4	18	4
19 July	1325–2300	10	55	109
4 August	0800–2000	9	40	61
9 August	0900–2015	9	37	31
11 August	1400–1900	10	61	274
Totals		70	353 (5.88 h)	894

nals is related to the degree of common orientation of the hydrometeors in the volume from which the backscatter is received, and the phase of the cross-covariance is related to the mean canting angle of the hydrometeors in the backscatter volume.

Propagation effects arise from anisotropy in the propagation medium and are defined relative to the principal axes of the medium. These axes correspond to the orientations at which linearly polarized signals experience maximum and minimum attenuation and phase shift in propagation. The effect of differential phase shift on a circularly polarized signal is to change its ellipticity, while the effect of differential attenuation is to change the shape of the initially square envelope of the maximum amplitudes relative to the principal axes. Either of these effects results in the progressive transfer of power from the initial polarization state to the orthogonal. The propagation effects are revealed most directly by the cross-covariance when it is normalized by the power received in the main channel to yield the cross-covariance amplitude ratio

$$\mathrm{CCAR} = \frac{\langle E_1 E_2^* \rangle}{\langle E_2 E_2^* \rangle}, \qquad (1)$$

where the brackets denote time averages of the complex products of the signals. The expected value of this quantity, derived originally by McCormick and Hendry (1975), is given by

$$E(\mathrm{CCAR}) = \rho_\alpha \bar{\nu} e^{i(\bar{\delta} \pm 2\bar{\alpha})} + 2pe^{i(\chi \pm 2\tau)} + 2\bar{\epsilon}. \qquad (2)$$

On the right side of Eq. (2) the first term, due to backscatter from each gated sample volume, includes the reflectivity-weighted average of the complex backscatter amplitude ratio $\nu e^{i\delta}$, the mean canting angle $\bar{\alpha}$ in the backscatter medium, and the effective fraction of oriented scatterers ρ_α. The upper and lower signs correspond to the transmission of right and left circular polarization, respectively. The second term, due to propagation, is based on a model of an anisotropic medium with symmetry axes rotated through an angle τ from the vertical and horizontal (McCormick and Hendry 1976); the parameters p and χ are related to the total one-way differential attenuation ΔA (dB) and differential phase shift $\Delta\Phi$ (deg) between the radar and each sampled range, to first-order approximation, by

$$pe^{i\chi} = \tanh\left[0.0575\Delta A + i\left(\frac{\pi}{360}\right)\Delta\Phi\right]. \qquad (3)$$

The third term of Eq. (2) represents the polarimetric error of the radar system averaged over the antenna radiation pattern.

When the backscatter and propagation terms are of similar magnitude, it is sometimes difficult to separate them. On the other hand, any consistent rangewise change of the CCAR generally indicates a propagation effect, regardless of the magnitudes of the terms. Temporal changes of any of the measurable quantities associated with changing electric fields (e.g., changes coincident with lightning) provide indications of the changing strength and direction of the field.

The rangewise change of the CCAR indicates propagation characteristics relative to the principal axes of the propagation medium. If the principal axes are horizontal and vertical [i.e., $\tau = 0$ in Eq. (2)], then the real part of the incremental CCAR is proportional to the differential attenuation and the imaginary part of the incremental CCAR is proportional to the differential phase shift, as implied by the formulation of the propagation term in Eq. (3). In this case, the respective quantities are positive if the attenuation and phase shift of a horizontally polarized signal are greater than the attenuation and phase shift of a vertically polarized signal, which are the usual conditions in rain.

Because the formulation of the CCAR incorporates the mean canting angle τ of the propagation medium, in general one must measure all four polarimetric backscatter amplitudes (i.e., the full polarimetric matrix) to derive all the propagation quantities. However, the interpretation is simplified in two cases. First, in rain, the mean canting angle is near 0°, and the CCAR

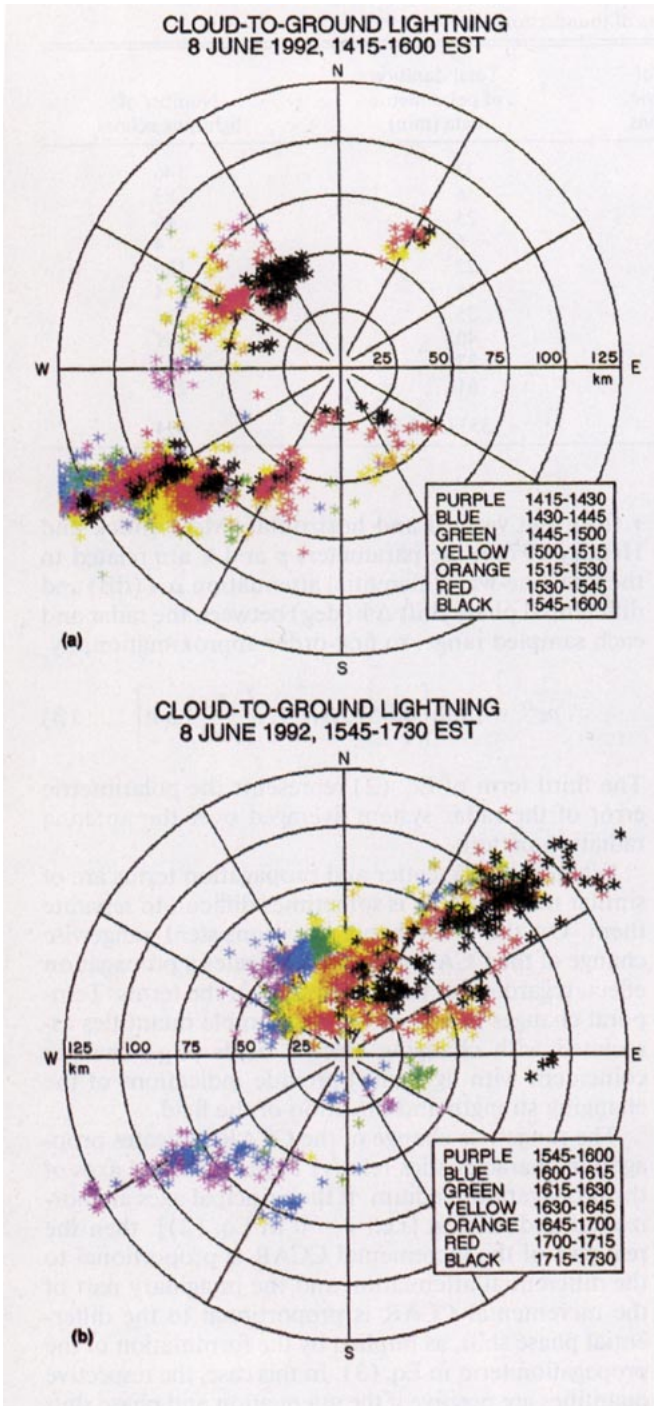

FIG. 1. Cloud-to-ground lightning recorded by the nationwide network on 8 June 1992 within 125 km of the radar. Earliest cells appeared due west of the radar about 1200 EST and moved eastward. Other cells developed northwest of the radar after 1400. (a) 1415–1600 EST. Storm A is near 235° azimuth and 100-km range at 1500–1515 (yellow) and near 230° azimuth and 85-km range at 1530–1545 (red). (b) 1545–1730 EST. Storm B is near 335° azimuth and 50-km range at 1600–1615 (blue), and storm C is near 330° azimuth and 35-km range at 1630–1645 (yellow).

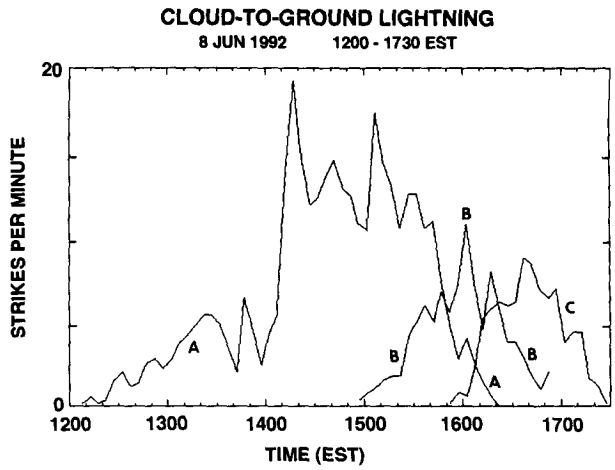

FIG. 2. Cloud-to-ground lightning in three storms recorded by the nationwide network on 8 June 1992. Ordinate is the average number of strikes per minute in each 5-min interval.

derived from a half-matrix measurement such as ours may be reliably interpreted in terms of the differential attenuation and differential phase shift. Second, in a medium comprising small ice particles, the differential attenuation is negligible, and the rangewise change of the CCAR may be ascribed entirely to differential phase shift. In this case, the orientation of the rangewise profile in the complex plane, relative to the positive imaginary axis, is equal to twice the mean canting angle of the propagation medium.

5. Observations

a. 8 June 1992

A few convective cells appeared almost due west of the radar shortly after 1200 EST. These moved eastward and continued a high level of electrical activity until about 1600. By 1430 new cells had developed to the north and northeast of the original cells; the electrical activity of one of the newer cells increased rapidly after 1530 as the older cells gradually weakened. Figure 1 shows cloud-to-ground lightning locations recorded within 125 km of our radar by the nationwide network. We recorded polarimetric observations of three storms, one of which persisted for more than 4 h and all of which produced significant numbers of cloud-to-ground lightning strikes. Figure 2 shows the electrical activity of these storms as recorded by the nationwide network. Surface temperatures in Massachusetts and northern Connecticut during the early afternoon were between 27° and 30°C, and dewpoint temperatures were between 19° and 22°C. The temperature soundings from Albany, New York, 195 km west-northwest of the radar, at 0700 EST (1200 UTC) and from Chatham, Massachusetts, 150 km east-southeast of the radar, at 1900 EST (0000 UTC 9 June) showed the

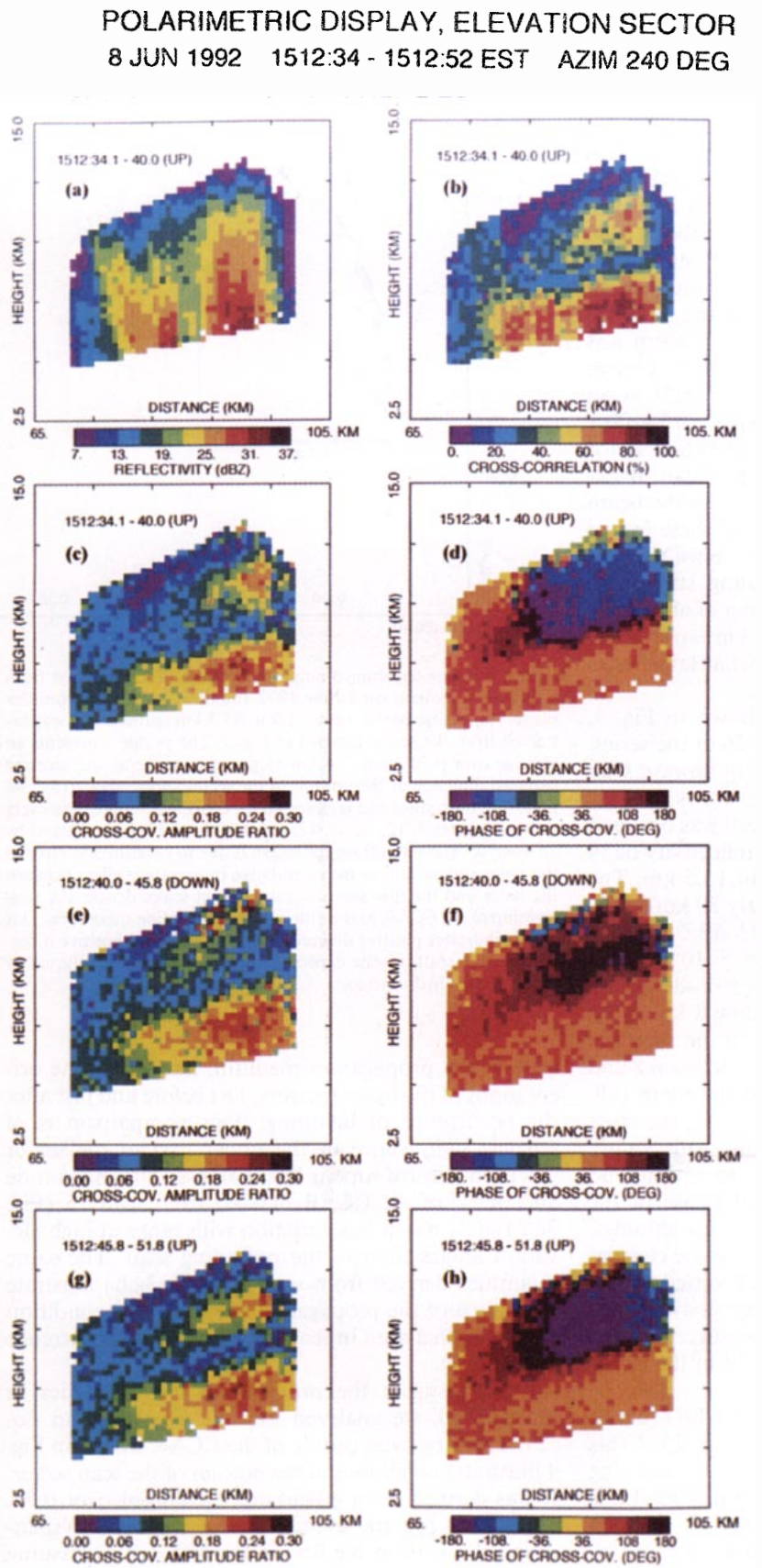

FIG. 3. Polarimetric radar observation of changing orientations of hydrometeors in response to changing electric field in storm A on 8 June 1992. Data were derived from elevation scans 24, 25, and 26 in the first observation of the storm. Top four panels show (a) reflectivity, (b) cross correlation, (c) magnitude of the cross-covariance amplitude ratio (CCAR), and (d) phase of the cross-covariance, all derived from scan 24. Panels (e) and (f) show the magnitude and phase of the CCAR derived from scan 25, and panels (g) and (h) show the same quantities derived from scan 26.

0°C isotherm near 4.3-km altitude. Winds at the surface were generally from the southwest at 3–5 m s^{-1} (5–10 kt). The wind veered to west-northwesterly at 8-km altitude with speed increasing to a maximum near 30 m s^{-1} (60 kt) at 12 km. The tropopause was at 15 km over Chatham but near 12 km over Albany.

The thunderstorm identified as storm A in Fig. 2 developed about 130 km west of the radar about 1230 EST and moved eastward at 15–20 km h^{-1} during the following 4 h. Because of our unsuccessful attempts to observe electrical effects at long range during 1991, we did not record polarimetric data until the storm was less than 100 km distant. We recorded the first series of polarimetric data from 1509:48 to 1515:21 at an azimuth of 240° with the gates set to span 70.7–100.1 km in range. The antenna scanned the elevation sector 4°–8° continuously at a rate of 5.9 s per scan. Backscatter from lightning channels intersecting the beam occurred at intervals of 2–13 s; many of these events exceeded 0.5 s in duration or spanned more than 10 km in range. Cloud-to-ground lightning strikes occurred at a rate of 13.6 min^{-1} in an area of about 500 km^2 centered at 235° azimuth and 90-km range; a few more strikes occurred within a somewhat larger area surrounding the radar gates.

Characteristics of this storm are shown in Fig. 3, based on data from scans 24, 25, and 26 of the series. The reflectivity derived from scan 24, an upward scan beginning at 1512:34.1 EST (Fig. 3a), shows the general structure of the storm. The main cell was centered at a range of 92 km with a maximum reflectivity of 34 dBZ and extended to a height of about 15.5 km. The rangewise extent of the storm was nearly 30 km at low altitude, and reflectivity in excess of 15 dBZ spanned a range interval of 25 km at altitudes of 8–10 km. The cross correlation (Fig. 3b) was highest (50%–80%) and nearly constant from scan to scan below 8 km in altitude in the main cell, probably due to the presence of liquid or water-coated hydrometeors. Between 8 and 11.5 km altitude in the upper part of the main cell, where the temperature was −25° to −55°C, the cross correlation varied from scan to scan, with values sometimes as high as 60%–80% and sometimes no higher than 40%. The magnitude and phase of the CCAR (Figs. 3c,d) were fairly constant at low altitudes, but above about 8 km they exhibited rangewise changes suggestive of propagation effects, which varied widely from scan to scan. Comparison of successive sector scans reveals cyclical effects related to successive increases and decreases of the electric field in the upper part of the storm.

A lightning echo occurred at 1512:40.1 EST, about 0.1 s after the start of the downward scan 25. [This was an unusually large and long-lived echo, spanning 11.4 km (20 gates) in range and continuing for 1.2 s; it is evident in the high values of the CCAR between 86 and 97 km in range near 12.5 km in altitude in Fig. 3e.] These two scans, thus, enable us to compare the state of the propagation medium, and hence the orientations of the hydrometeors, just before and just after the occurrence of lightning. This comparison is of greatest significance in the upper part of the sector where the return time is less than 6 s. The magnitude and phase of the CCAR derived from scan 25 (Fig. 3e,f) show much less variation with range at high elevation angles than in the preceding scan. The same quantities derived from scan 26 (Fig. 3g,h) illustrate the return of the propagation medium to a condition similar to that seen in scan 24, prior to the occurrence of lightning.

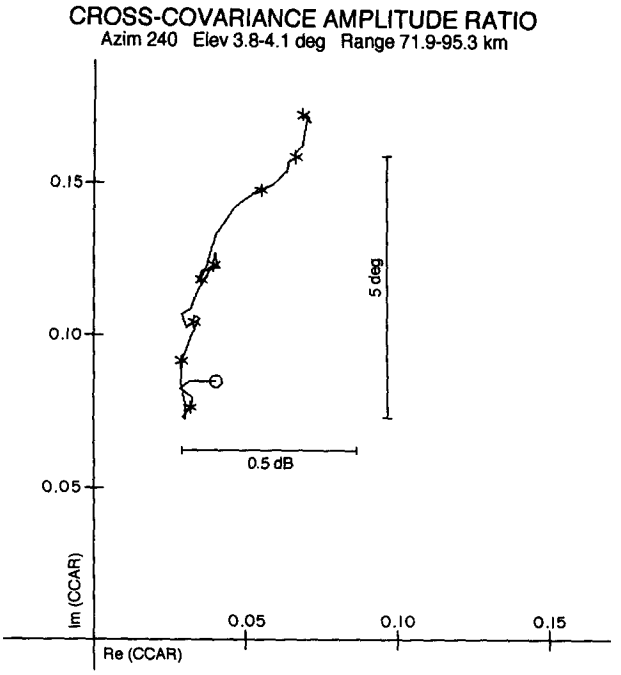

FIG. 4. Cross-covariance amplitude ratio (CCAR) derived from radar measurements on 8 June 1992 and displayed on the complex plane. Rangewise profile from 71.9 to 95.3 km (gates 3–42) was extracted from the scans depicted in Fig. 3. The profile represents an average over 0.70 s and 2.4 km (5 gates) in range as the antenna reversed direction at the bottom of the second scan, about 1512:46 EST. The near-range end is closest to the coordinate origin, and every fifth gate (gates 7, 12, . . . , 42, at intervals of 3 km) is marked by an asterisk. The offset from the origin is due to polarimetric error in the radar system and to the cumulative propagation effect between the radar and the first sampled range. Inset scales denote the relationship of the CCAR to the differential propagation quantities. This profile indicates positive differential attenuation and positive differential phase shift, as one expects in propagation through liquid or liquid-coated hydrometeors.

To investigate the propagation characteristics in more detail, we analyzed the CCAR defined in Eq. (2). The rangewise profile of the CCAR shown in Fig. 4 illustrates conditions at the bottom of the scan sector. It was derived from covariances averaged over 0.7 s and from a moving average of five range gates (spanning 2.4 km from the first to the fifth). If we assume that the mean canting angle is zero near the bottom of

the scan sector, as would be true for hydrometeors that are liquid or liquid-coated, then the change of the CCAR in Fig. 4 between its extreme values at 74.9 and 95.3 km (gates 8–42) indicates a total differential attenuation of 0.35 dB, or an average of 0.017 dB km^{-1}, and a total differential phase shift of 5.7°, or 0.28° km^{-1}. At low elevations there was no significant change of the profile of the CCAR from scan to scan, even at intervals of tens of seconds. The observed orientation of the CCAR, slightly clockwise from the positive imaginary axis, provides assurance that the phase calibration of the two receiver channels is approximately correct. Any residual phase imbalance between the two channels would rotate the CCAR in the complex plane and bias the derived values of differential attenuation or differential phase shift.

We investigated the changes at high altitude by examining rangewise profiles of the CCAR computed in the elevation sector 6.3°–6.7°, where the propagation effects were greatest. Several of the lightning discharges occurred at times that permitted comparison of the propagation effects observed immediately before and immediately after. Figure 5 shows profiles of the CCAR associated with three of these events. The interpretation of the CCAR at these heights (8.1–10.8 km, where the temperature is −25° to −50°C) relies on the assumption that the propagation medium comprises lossless ice particles. In each case, the differential phase shift is relatively large just before the occurrence of lightning, much smaller a few seconds after, and large again several seconds later. Each sequence indicates a relatively high degree of orientation of the hydrometeors in the propagation medium before the lightning, a lower degree of orientation immediately after, and a restoration of the highly oriented state within several seconds.

The profiles in the third panel of Fig. 5 are derived from the scans shown in Fig. 3. The first profile in the third panel of Fig. 5, centered 2.6 s before the lightning, yields a total differential phase shift of 11.7° between 74.3 and 95.3 km (gates 7–42), or 0.56° km^{-1}, and a mean canting angle of 75° counterclockwise. The second profile, centered 1.9 s after the lightning, yields a total differential phase shift of about 5.2° between 71.9 and 82.1 km (gates 3–20), or 0.51° km^{-1}, and a mean canting angle of about 45° counterclockwise. Beyond gate 20 the orientation of the CCAR is similar to that observed before the lightning. However, the incremental differential phase shift is much less and indicates that the hydrometeors are more randomly oriented than before the lightning. The third profile, 9.2 s after the lightning, indicates that the propagation medium at nearly all ranges has returned to an oriented state similar to that which existed before the lightning.

We calculated from each profile the specific differential phase shift (° km^{-1}) between 74.3 and 92.3 km (gates 7 and 37), the ranges between which the direction of the CCAR was most nearly uniform when the propagation effect was largest. The resulting data are

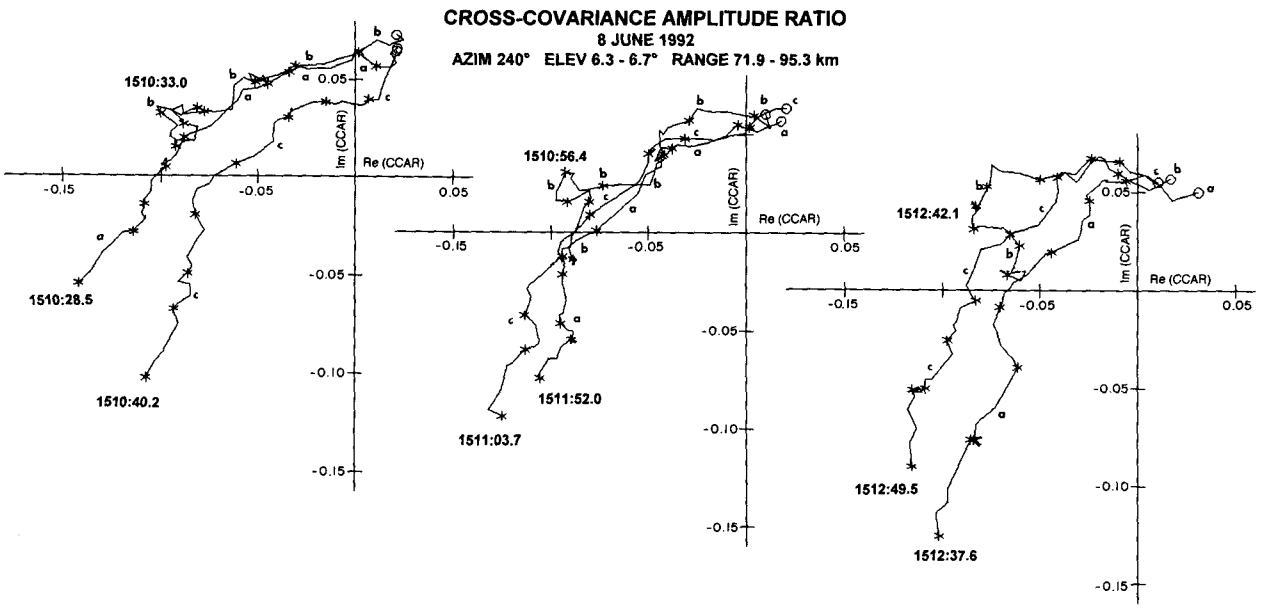

FIG. 5. Rangewise profiles of the cross-covariance amplitude ratio (CCAR) in storm A on 8 June 1992. Profiles represent averages over 0.56 s as the antenna moved between 6.3° and 6.7° elevation and 2.4 km (five gates) in range. The center points of the five-gate averages span the range interval of 71.9–95.3 km (gates 3–42). The near-range end of each profile, in the upper-right quadrant in each case, is marked by a circle. Every fifth gate (7, 12, . . . , 42, at intervals of 3 km) is marked by an asterisk. The offset from the origin is due to polarimetric error in the radar system and to the cumulative propagation effect between the radar and the first sampled range. The center time (EST) of the averaging interval is displayed near each profile. Each set of three profiles comprises observations (a) a few seconds before a lightning discharge, (b) 1–2 s after, and (c) 8–9 s after. Lightning discharges occurred at 1510:32.1, 1510:54.5, and 1512:40.1 EST.

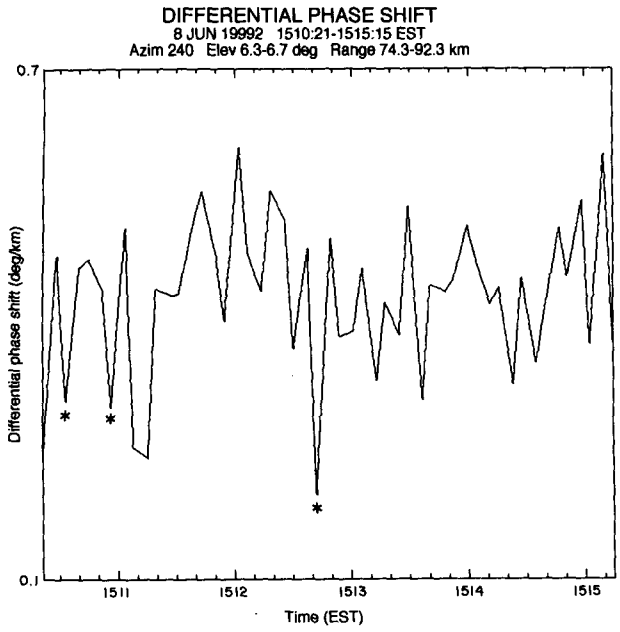

FIG. 6. Variations in specific differential phase shift associated with lightning in the first observation of storm A on 8 June 1992. Phase shift is computed in the elevation interval of 6.3°–6.7° and the range interval of 74.3–92.3 km. Most of the large changes (greater than about 0.2° km^{-1}) are unambiguously associated with lightning discharges. The minima at 1510:33.0, 1510:56.4, and 1512:42.1, marked by asterisks, correspond to the profiles labeled "b" in Fig. 5.

shown in Fig. 6. Nearly all the large decreases are associated with occurrences of lightning. We related these data to the changing electric field by means of the scatterplots shown in Figs. 7 and 8. In these figures each measurement of the specific differential phase shift is plotted according to the time increment by which it either preceded (Fig. 7) or followed (Fig. 8) an occurrence of lightning in the radar beam. The significance of each associated lightning event was estimated and categorized according to its duration, rangewise structure, and intensity; the four categories contain events of durations and rangewise extents as follows: 1) 0.1–0.3 s, 1–5 gates; 2) 0.2–0.5 s, 2–11 gates; 3) 0.2–1.1 s, 2–25 gates; and 4) 0.5–1.2 s, 3–29 gates.

The data in Fig. 7 reveal a general tendency of increasing specific differential phase shift prior to an occurrence of lightning. The apparent rate of increase is about 0.05° km^{-1} s^{-1} to a maximum value near 0.55° km^{-1}. Several pairs of successive observations illustrate this increase distinctly; these include 20–21, 23–24, 30–31, 32–33, 40–41, and 44–45. Some observations, such as 17, 18, 37, and 38, do not constitute related pairs, as they precede different lightning events. Nevertheless, these observations are consistent with the general pattern of increasing propagation effect prior to the occurrence of lightning. The identification of lightning echoes is critical to the development of a statistical relationship between a measurable quantity and the time to an occurrence of lightning. In some cases, especially with widely spaced range gates, an occurrence of lightning may be missed or may appear only faintly in the radar signal. Such an event may have occurred a few tenths of a second after observation 33. If it were included, then observations 32 and 33 would both be displaced to the right in Fig. 7 by about 6 s.

The characteristics of the specific differential phase shift after an occurrence of lightning are not as well-defined. Figure 8 indicates that although small values of the phase shift are observed only within a few seconds after lightning, there is often only a slight decrease of the phase shift after lightning. Figure 8 suggests that after lightning, the phase shift increases rapidly at first and then more slowly; other observations support this suggestion.

We recorded the second observation of this storm about 25 min later, scanning the elevation sector 4°–8° at an azimuth of 231°. Backscatter from lightning channels intersecting the beam occurred at intervals of 2–22 s, but generally less frequently than during the first observation. Cloud-to-ground strikes occurred at 5 min^{-1}. The radar detected two cells within the storm centered at 75 and 84 km in range; the storm extended

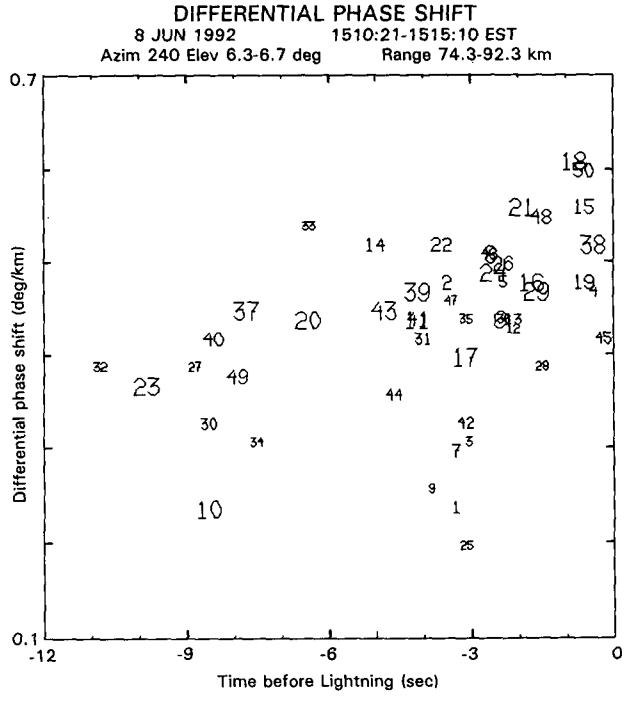

FIG. 7. Scatterplot of specific differential phase shift (from Fig. 6) and time by which the radar measurement preceded an occurrence of lightning. Numbers denote sequential observations of the elevation sector. Data are stratified in four categories denoted by size of the plotted observation number according to the significance of the nearest following lightning event estimated from its duration, rangewise structure, and signal strength. The data associated with the most significant lightning events reveal a consistent increase of the propagation effect prior to the occurrence of lightning.

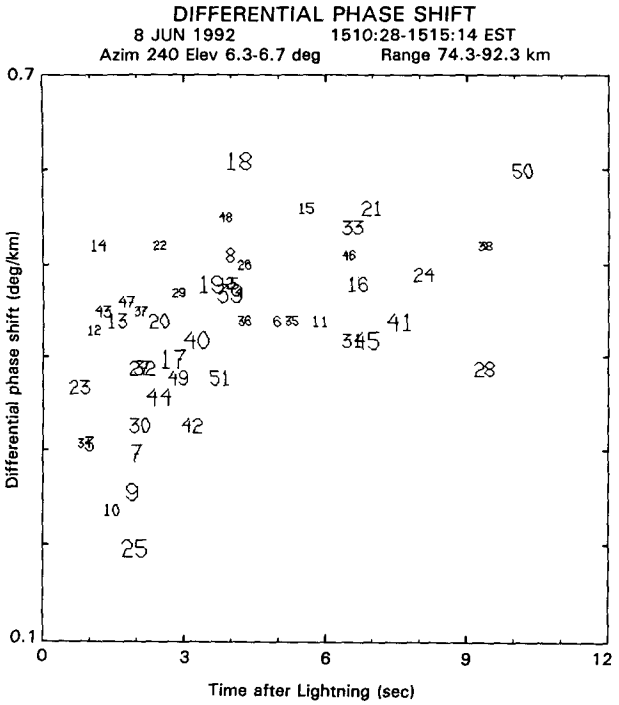

FIG. 8. Scatterplot of specific differential phase shift (from Fig. 6) and time by which the radar measurement followed an occurrence of lightning. Plot characteristics are identical to those of Fig. 7, except that data are stratified according to the significance of the nearest preceding lightning event. The relationship is not as well defined as in Fig. 7.

to a height of 13 km. As in the previous observation, the CCAR exhibited changes from scan to scan in the upper part of the cells. The specific differential phase shift attained values up to 0.6° km^{-1}, comparable to those derived from the first observation, indicative of continuing strong electric fields, and the relative changes from scan to scan were comparable to those seen previously, especially during the first half of the observation. However, the maximum propagation effect occurred at a lower altitude (7.7–8.5 km) and in a smaller range interval (about 8 km) than in the first observation, and the changes were not as well correlated with the occurrence of lightning. These differences may be associated with the lower level of electrical activity of the storm. If the spatial extent of these effects perpendicular to the beam is comparable to their limited rangewise extent, then the observational result is particularly sensitive to the choice of azimuth, which may not have been optimum.

We observed two other storms on 8 June. Storm B (Fig. 2) developed 70 km west-northwest of the radar after 1500 EST and moved east-northeastward at 50 km h^{-1}. We recorded two series of polarimetric data as the storm passed within about 50 km of the radar. Cloud-to-ground strikes were recorded at a rate of about 8.3 and 4.3 min^{-1} during these series. We calculated specific differential phase shifts up to 0.5° km^{-1} in range intervals of 8–9 km at altitudes of 7–11 km, but there were no sudden changes that could be associated with lightning.

Storm C (Fig. 2) developed about 30 km northwest of the radar about 1600 EST and moved northeastward at 30 km h^{-1}. We recorded three series of polarimetric data, the first of which coincided with the maximum rate of cloud-to-ground strikes, 7.9 min^{-1}. The first of these series revealed a specific differential phase shift that varied between 0.1° and 0.6° km^{-1} in a 5-km range interval at heights of 7–8 km along the radar beam. Although several sharp decreases of the phase shift were obviously associated with lightning, the series as a whole showed only slight correlation of the phase shift with time either before or after lightning. During the subsequent observations, the electrical activity was decreasing and the maximum specific differential phase shift was only about 0.3° km^{-1} in a range interval of about 7 km. Changes of the CCAR coincident with two lightning events indicated changes of 5°–15° in the mean canting angle over a range interval of about 15 km. Although the changes were only slight, the differential propagation effects revealed a persistent anisotropy of the medium that is indicative of a persistent electric field in the cloud.

b. 20 June 1992

We recorded eight data series while observing seven different storms between 1403 and 1722 EST, mostly north and west of the radar. Individual cells moved eastward at speeds of 25 km h^{-1} or less. Although the slow movement was advantageous for our observations, none of the storms was very active electrically. Durations of these storms ranged from 1 to 3.5 h, and the maximum rate of cloud-to-ground lightning was about 4 min^{-1} in the most active storm, which was not the longest-lived. Surface temperatures in eastern Massachusetts during the early afternoon were 22°–25°C, and dewpoint temperatures were 17°–20°C. The temperature sounding from Chatham, Massachusetts, at 0700 EST (1200 UTC) showed the 0°C isotherm at an altitude of 3.7 km and the tropopause at 12.6 km. Winds at the surface were generally from the south or southwest at 3–5 m s^{-1} (5–10 kt) during the early afternoon. Winds aloft were southerly or southwesterly at all heights with a maximum speed of 40 m s^{-1} (78 kt) at 8.2 km.

Three of these storms exhibited no differential propagation effects, primarily because the backscattered signals were too weak. Two storms early in the afternoon exhibited propagation effects, but each exhibited only one sudden change coincident with lightning. In one of these, about 48 km distant, we observed a specific differential phase shift of 1°–1.2° km^{-1} in a range interval of 3.9 km at altitudes of 7.1–7.7 km. After the occurrence of lightning, the phase shift was immedi-

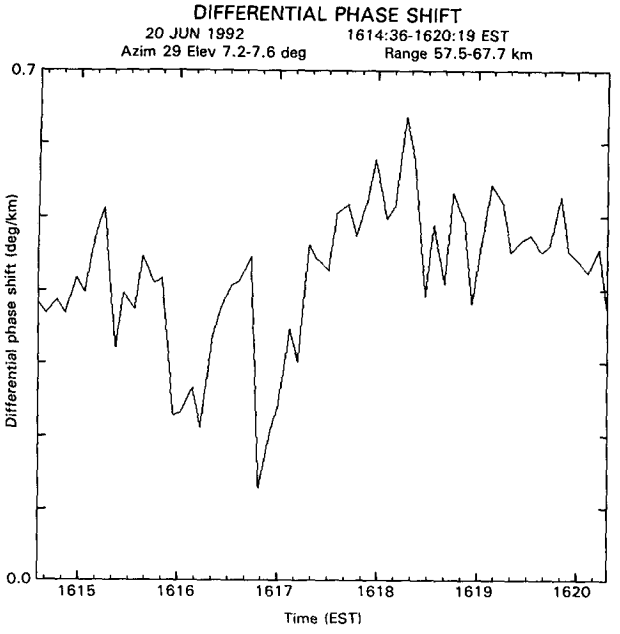

FIG. 9. Variations in specific differential phase shift associated with lightning in the fifth storm on 20 June 1992. Phase shift is computed in the elevation interval of 7.2°–7.6° and the range interval 57.5–67.7 km (gates 16–33). Deep minima correspond to reduced propagation effect through the entire range interval; shallow minima are due to reduction of the propagation effect in only part of the interval.

ately reduced to 0.55° km^{-1} and was restored in about 25 s. In the most active storm on this day we observed two cells, at ranges of 84 and 98 km, and a specific differential phase shift of 0.47° km^{-1} in a range interval of 4.8 km at altitudes of 7.2–7.6 km in the nearer of the two cells. After one large lightning event (7 km in range and 0.5 s duration) the phase shift was reduced to 0.13° km^{-1}, remained low for about 30 s, and then increased gradually to regain its original value about 1 min after the lightning event. In a second observation of this storm, about 40 min later, we detected no propagation effects.

Three storms late in the afternoon exhibited strong propagation effects with cyclical variations associated with lightning. All of these were relatively short-lived (the duration of cloud-to-ground lightning in these storms was between 1 h 20 min and 1 h 50 min), and we observed each of them only once. We observed the first of these storms about 60 km northeast of the radar from 1614:28 to 1621:32 EST, just after the peak of its electrical activity as the rate of cloud-to-ground lightning was decreasing from 3 to 1 min^{-1}. The radar scanned the elevation sector 5°–9° at 5.8 s per scan with the range gates spanning the interval of 49.1–78.5 km. The maximum reflectivity at the bottom of the scan sector, at an altitude of 5 km, was 23 dBZ at 61-km range. The reflectivity exceeded 10 dBZ in a range interval of 7 km at altitudes of 7–10 km. The propagation effect persisted in the altitude range of 7–10 km throughout the observation, although it decreased somewhat after 1619. We analyzed the subsector 7.2°–7.6° in the same manner as described above for the observations of 8 June. Figure 9 shows the specific differential phase shift in the range interval of 57.5–67.7 km, spanning altitudes of 7.4–8.7 km. The four largest decreases, and several of the smaller ones, are associated with lightning echoes detected by radar. The recovery times of the differential phase shift are about 25–40 s, much longer than those observed in the most active storm on 8 June. Figures 10 and 11 are scatterplots of the specific differential phase shift and the time by which each observation preceded or followed a lightning event. Figure 10 shows a distinct tendency of increasing phase shift up to the time of a lightning discharge, with a rate of about 0.007° km^{-1} s^{-1} to a maximum of about 0.55° km^{-1}. Figure 11 indicates a similar rate of increase of the phase shift after lightning.

The second of the later storms comprised three cells 43–55 km northwest of the radar during our observation from 1639:39 to 1649:30 EST. The observation time was near the end of its peak electrical activity, while the rate of cloud-to-ground lightning was about 2 min^{-1}. The radar scanned the elevation sector 5°–12° at 10 s per scan with the range gates spanning the interval of 41.7–71.1 km. We analyzed the CCAR in

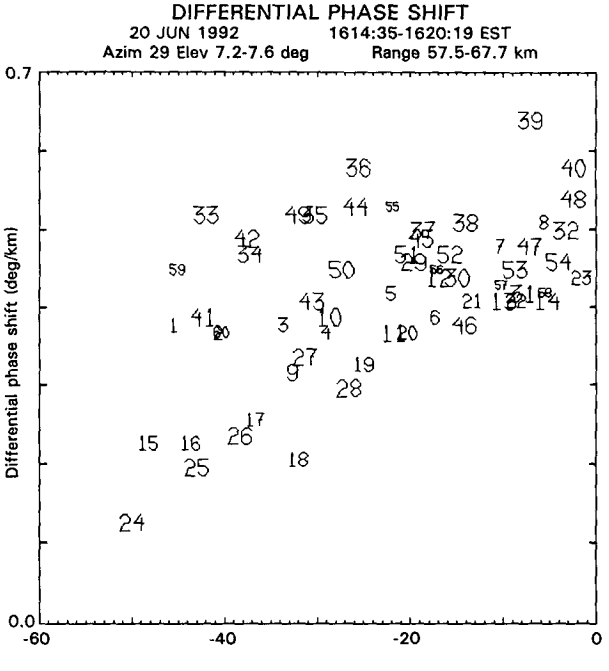

FIG. 10. Scatterplot of specific differential phase shift (from Fig. 9) and time by which the radar measurement preceded an occurrence of lightning. Numbers denote sequential observations of the elevation sector. Data are stratified in four categories, denoted by size of the plotted observation number, as in Fig. 7. The increase of the propagation effect prior to the occurrence of lightning is more distinct than in Fig. 7 but occurs on a longer timescale.

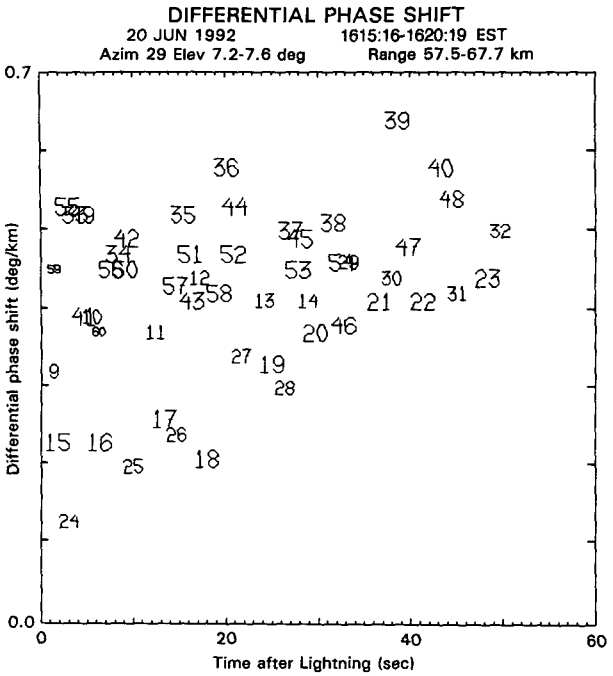

FIG. 11. Scatterplot of specific differential phase shift (from Fig. 9) and time by which the radar measurement followed an occurrence of lightning. Plot characteristics are identical to those of Fig. 10, except that data are stratified according to the significance of the nearest preceding lightning event.

the subsector 8.8°–9.2° and extracted the specific differential phase shift in an interval of 9 km nearly centered above the three cells at altitudes of 7.2–8.6 km. The maximum value was 0.43° km^{-1}, and there were two sudden decreases to about 0.2° km^{-1} after occurrences of lightning.

We observed the third storm 85 km north of the radar from 1710:43 to 1722:20 EST, just after its peak of electrical activity as the rate of cloud-to-ground lightning was decreasing from nearly 3 min^{-1} to just below 2 min^{-1}. During most of this observation, the radar scanned the elevation sector 2°–7° at 7.3 s per scan with the range gates spanning the interval of 70.2–99.6 km. Although lightning echoes were infrequent (about 2 min^{-1}), we detected strong propagation effects and several sudden decreases coincident with lightning. We analyzed the CCAR in the subsector 5.2°–5.6° and extracted the specific differential phase shift in a range interval of 72.0–89.4 km, which spanned most of the upper part of the storm at altitudes of 6.8–8.4 km. The reflectivity at this elevation angle was greater than 10 dBZ for a range interval of about 18 km, with a maximum of 18 dBZ near 7.5-km altitude. The specific differential phase shift varied between 0.1° and 0.8° km^{-1} and exhibited characteristics similar to those of the series shown in Fig. 10. A scatterplot in the format of Fig. 10 showed that the specific differential phase shift increased at about 0.007° km^{-1} s^{-1} to a maximum of about 0.75° km^{-1} before each occurrence of lightning.

c. *11 August 1992*

Thunderstorms developed during the afternoon along a line that was oriented west-southwest to east-northeast and that initially nearly bisected our surveillance area. The line moved very slowly to the south-southeast, and by 1720 EST was about 70 km south-southeast of the radar site. Individual cells moved eastward, mostly at speeds of 40–70 km h^{-1}. Lightning generated by three of these storms and recorded on the nationwide network is shown in Fig. 12. Surface temperatures in Boston and at nearby reporting stations during the early afternoon were 28°–32°C, and dewpoint temperatures were 19°–23°C. The temperature soundings from Chatham, Massachusetts, at 0700 EST (1200 UTC) and at 1900 EST (0000 UTC 12 August), showed the 0°C isotherm at altitudes of 4.2 and 4.7 km, respectively, and the tropopause at 13.1 and 14.5 km, respectively. Winds at the surface were generally from the west or northwest at 5–10 m s^{-1} (9–18 kt) during the early afternoon. The wind above 7 km was southwesterly with a maximum speed of 22 m s^{-1} (43 kt) at 10 km.

We observed two storms early in the afternoon, including one (storm A in Fig. 12) that developed close to the radar about 1330. Both of these were small and weakening during our observations and yielded no evidence of changing particle orientations related to lightning.

An area of convective activity developed about 35 km southeast of the radar about 1400 EST and moved eastward at 25 km h^{-1}. This area, identified as storm B in Fig. 12, initially comprised a series of small cells,

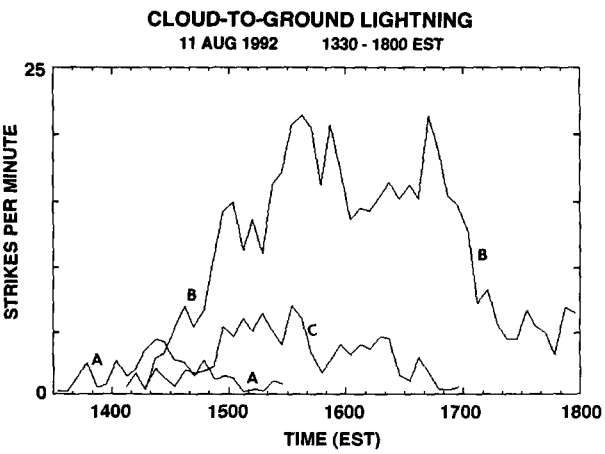

FIG. 12. Cloud-to-ground lightning in three storms recorded by the nationwide network on 11 August 1992. Ordinate is the average number of strikes per minute in each 5-min interval. Storm B produced more lightning than any other that we observed in 1991 or 1992.

each of which moved eastward faster than the area as a whole. After 1600 EST, one cell became dominant but assumed the relatively slow eastward movement that had characterized the overall system from its inception. The maximum rate of cloud-to-ground lightning strikes was 21 min^{-1} within an area of about 1000 km^2 about 1535 EST. Electrical activity decreased slowly thereafter and more rapidly after 1700 to about 6 min^{-1} when the storm was about 80 km distant. Between 1439 and 1715 EST, we recorded seven series of polarimetric data from this storm. The rate of cloud-to-ground lightning exceeded 6 min^{-1} during all of these and exceeded 10 min^{-1} during five of them. The first two observations (1439:52–1448:10 and 1449:35–1456:31) revealed only slight propagation effects. The third series (1516:41–1522:59) showed specific differential phase shifts of 0.34–0.55° km^{-1} between a 62.6 and 71.0-km range at 6.5° elevation (7.1–8.0 km in altitude), but the signal levels in the region of interest were too low (equivalent reflectivity factor 5–15 dBZ) to permit detailed analysis. The fourth observation (1559:07–1606:11) was made just after the peak of the cloud-to-ground lightning. The echo top height was 13 km during this observation, and reflectivity above 10 dBZ spanned nearly 13 km in range at an altitude of 8 km. Although the radar detected 37 lightning echoes, there was an interval of 75 s during which no lightning echoes were detected. A propagation effect was evident during most of the observation, with specific differential phase shifts of 0.3°–0.4° km^{-1} between 70 and 81 km in range at an elevation angle of 6° (7.3–8.4 km in altitude). The phase shift changed only slightly from scan to scan, and there were no changes that were obviously related to the occurrence of lightning. During the fifth observation (1624:04–1629:47), two cells moved through the scan plane. One of these exhibited a maximum reflectivity of 45 dBZ, the highest we observed on this day, and a top height of 13.75 km. The radar detected 54 lightning echoes during the 5.7-min observation. A propagation effect at elevation angles of 5°–6° was strongest during the first 3 min of the observation. Although the derived values of the specific differential phase shift ranged from 0.2°–1.4° km^{-1} in the range interval of 85.5–89.1 km at 5.5° elevation (8.2–8.5 km in altitude), the changes from scan to scan were generally slight.

The sixth observation of storm B (1648:49–1656:14) was made just after the final peak of the cloud-to-ground lightning shown in Fig. 12 and proved to be the most interesting. The electrical activity during this observation, as indicated both by the rate of cloud-to-ground lightning (16.9 min^{-1}) and by the detection of 77 lightning echoes by radar, was higher than during any other of our observations. We scanned the elevation sector 3°–9° at a rate of 8.7 s per scan with the range gates spanning the interval of 73.7–96.2 km. The main cell had a maximum reflectivity of 27 dBZ at 86-km range and a rangewise extent of 16 km at low altitude. Reflectivity in excess of 15 dBZ spanned a range interval of 12 km at altitudes of 8–10 km, where the CCAR revealed a distinct propagation effect. This effect was centered near 7° elevation angle in scans 1 and 2, descended to about 6° by the time of scan 10, and persisted at that elevation thereafter. We analyzed it by computing successive profiles of the CCAR in the elevation sector 5.8°–6.2°. Profiles of the CCAR de-

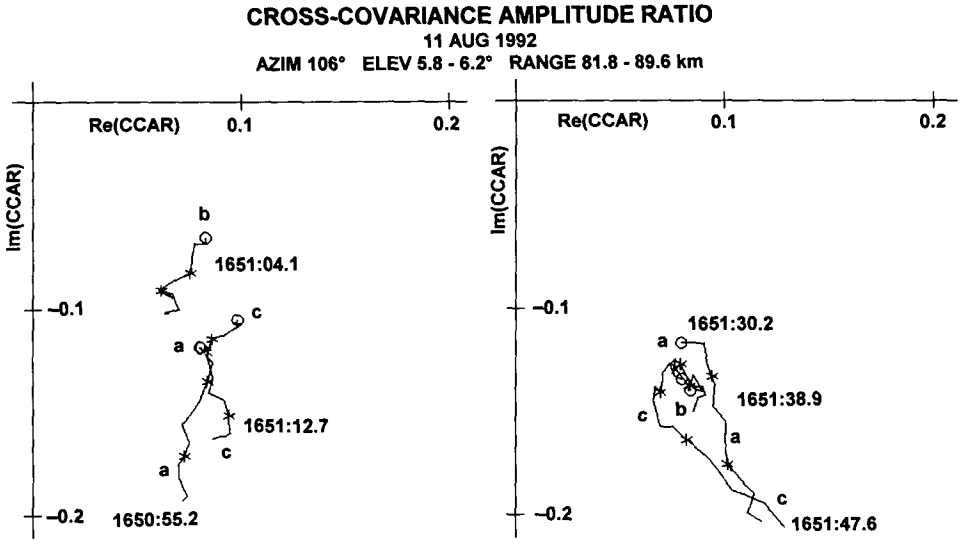

FIG. 13. Rangewise profiles of the cross-covariance amplitude ratio (CCAR) from the sixth observation of storm B on 11 August 1992. Profiles were derived from scans 15–17 (left) and scans 19–21 (right) in the elevation interval of 5.8°–6.2°, through the center of the maximum propagation effect, and are based on averages in time intervals of 0.55 s smoothed over 2.4 km (five gates) in range. Notation is similar to that in Fig. 5.

rived from scans 15–17 and scans 19–21 are shown in Fig. 13. The orientation of the CCAR in scan 17 implies a canting angle near 90° before lightning. Between scans 17 and 19 the apparent canting angle changed to about 80°, and scan 21 implies a canting angle of about 70°. The specific differential phase shift derived from this elevation sector in the range interval of 81.8–89.6 km is shown in Fig. 14. The initial values of specific differential phase shift in the sector were small because the propagation effect was initially concentrated at higher altitudes. After several seconds, the phase shift increased and ultimately attained values up to 1° km^{-1} with many sharp decreases associated with lightning. There were some differences between this case and that of storm A on 8 June. The range domain of the propagation effect and the relative change of the phase shift associated with lightning were generally less, and the specific differential phase shift showed no discernible correlation with the time by which the measurement preceded or followed the occurrence of lightning echoes. The most obvious reason for the latter result is the very frequent occurrence of lightning echoes and our inability to uniquely associate the lightning discharges with the observed changes in the propagation medium.

The seventh observation of storm B (1710:51–1715:02) occurred as the electrical activity was decreasing. We attempted to encompass two widely separated cells by spacing the range gates at 1.2 km but observed no propagation effects. This failure may be due either to the decreasing electrical activity or to the inadequacy of the wide spacing of the gates.

The storm identified as storm C in Fig. 12 developed about 40 km south of the radar about 1415 EST and moved eastward at 20 km h^{-1} during the following 2.5 h. The rate of cloud-to-ground lightning reached a maximum of 6.8 min^{-1} within an area of about 300 km^2 about 1535 EST. We recorded polarimetric data from 1538:31 to 1544:55 EST just after the peak of electrical activity in this storm. The antenna was pointed toward an azimuth of 128° and scanned the elevation sector 4°–12° at a rate of 11.2 s per scan, and the range gates were set at 35.5–64.9 km. The reflectivity aloft was initially high, up to 22 dBZ near 8-km altitude, where reflectivity greater than 10 dBZ spanned about 8 km in range. The early scans in the series revealed a strong propagation effect centered near 10.5° elevation with a specific differential phase shift of 1.1° km^{-1} extending from 43.8 to 54.0 km (heights of 8.0–9.8 km). The radar detected 15 lightning echoes during 6 min. Two of these, early in the observation, coincided with sharp reductions of the propagation effect. The differential phase shift was partially restored thereafter, but there was little or no change of the CCAR at a high altitude during the remainder of the observation, despite repeated detection of lightning by the radar.

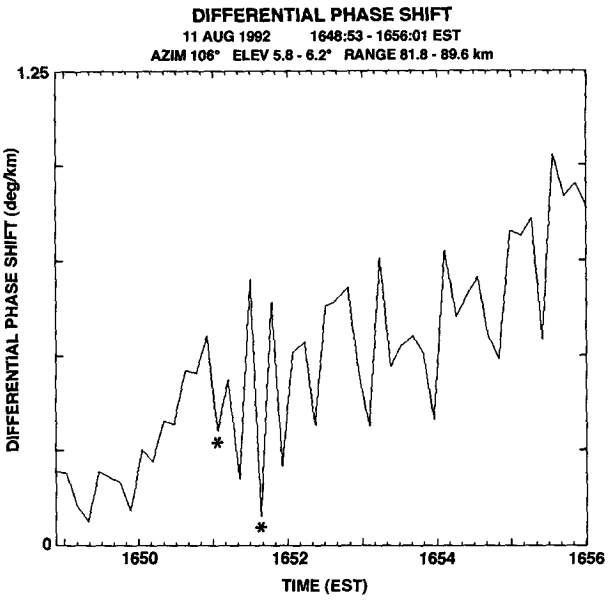

FIG. 14. Variations in specific differential phase shift associated with lightning in the sixth observation of storm B on 11 August 1992. Phase shift is computed in the elevation interval of 5.8°–6.2° and the range interval of 81.8–89.6 km (gates 20–33). Initial low values are due to the initial occurrence of the propagation effect at higher elevation angles. Subsequent large variations are probably associated with variations of the electric field, but these data are not well correlated with the observed lightning echoes. The minima at 1651:04.1 and 1651:38.9 EST, marked with asterisks, correspond to profiles labeled "b" in Fig. 13.

d. Other days

We recorded polarimetric data while observing thunderstorms on 7 other days during 1992. One observation on 9 August yielded results comparable to those of 20 June described above. On 19 July we observed an approaching squall line repeatedly. Propagation effects were absent or slight in all but one of these observations; in that one we derived a specific differential phase shift of 1.6° km^{-1} in a range interval of 3.3 km. In several other cases propagation effects were evident in the upper regions of storms but either were weak or did not exhibit changes related to lightning. In cases that exhibited little or no propagation effect, the observed storm was either weaker in reflectivity, smaller in vertical or horizontal extent, or much less active electrically than the most active storms on 8 June, 20 June, and 11 August. Rates of cloud-to-ground lightning were generally less than 5 min^{-1} in all of these storms and often as little as 1–2 min^{-1}, and lightning echoes detected by radar were similarly infrequent. As with the observations described previously, we operated mainly in the range domain of 40–100 km. The lack of observations at close range leaves open the possibility that propagation effects such as we observed on 8 June, 20 June, and 11 August might be observable in weak storms at closer range.

6. Discussion

a. Summary of observations

We observed changing propagation effects associated with rapidly changing orientations of hydrometeors in thunderstorms on several days during 1992. The observed effects occurred at altitudes of 7–11 km and were consistent with observations reported by other investigators. In many instances the observed changes could be related to occurrences of lightning that were detected by the radar. Observations of the most active storm on 8 June, for example, indicated that the specific differential phase shift due to propagation through ice particles increased repeatedly to a maximum value of about 0.55° km^{-1} in a range interval of 18 km and then decreased suddenly at the time of a lightning discharge. In other storms, we occasionally observed larger specific differential phase shifts, up to about 1.6° km^{-1}, within range intervals less than 10 km. On 8 June we observed a substantial reduction of the differential phase shift following an occurrence of lightning only when the radar beam traversed the upper part of the storm within 2–3 s after the lightning. When this region was not observed until 5–6 s after lightning, as was the case when lightning occurred during the lower half of a downward scan, the following scan typically indicated little or no change in the propagation medium, relative to its condition before the lightning. Such observations suggest that the electric field was substantially restored within that time. On 20 June the restoration of the electric field occurred more slowly.

Previous observations of this type (e.g., Hendry and McCormick 1976) have shown two modes of cyclical change of the cross correlation. The cross correlation may either increase gradually between lightning discharges and decrease suddenly coincident with the discharge or decrease gradually and increase suddenly. Hendry and McCormick suggested that the latter mode of change is due to a sudden return of the ice particles to an aerodynamically oriented state (i.e., a mean canting angle of 0°) following a sudden decrease of the electric field. Because small ice particles are nearly lossless, even for signals of wavelength much shorter than ours, such an oriented state would yield a rangewise profile of the CCAR that lay parallel to the positive imaginary axis in the complex plane. Hendry and Antar (1982) presented an observation that may indicate a sudden return to an aerodynamically oriented state. We rarely observed such an orientation of the CCAR at high altitudes in thunderstorms. Observations such as those shown in Figs. 5 and 13 imply that the particles did not become aerodynamically oriented after the occurrence of lightning. In some range increments, however, the incremental magnitude of the propagation term increased coincident with lightning, implying a local increase in the electric field.

b. Operational limitations

Several factors limited our ability to detect rapidly changing orientations of hydrometeors associated with changing electric fields in many of the storms we observed. Observational procedure is a fundamental issue. In our 1991 observations we usually aimed the radar beam to intersect a cell between 6 and 8 km in altitude, well above the melting level but low enough that the hydrometeor backscatter in each channel was well above the receiver noise level. Having observed propagation effects predominantly above 8 km in altitude in 1992, we believe that our observational technique in 1991 was largely responsible for our observing relatively few changes of polarimetric quantities coincident with lightning. The limited spatial domain of the observed propagation effects, both in height and in range in many cases, implies that the choice of azimuth and elevation angles is critical. The trade-off between the observed spatial domain and the scan cycle time is more severe at close range because one must scan a larger angular sector to observe a particular domain of height. The increased azimuthal component of storm motion at close range limits the time during which a storm can be observed effectively at a particular azimuth. A real-time display of polarimetric quantities, such as that developed by Rison et al. (1993) and used by Krehbiel et al. (1992, 1994), is of great value because it permits rapid evaluation and optimization of observational parameters. A second radar, operated continuously in a surveillance mode, would also aid polarimetric observations of storms, especially at close range, by providing timely and accurate guidance for optimum pointing of the polarimetric radar beam and optimum setting of range gates.

The electrical activity of a storm appears to be a significant factor. On 8 June and 11 August, for example, the storms that exhibited substantial and repeated changes of propagation effects were much more active electrically than any others we observed on those or other dates. In the later storms on 8 June, we observed few lightning echoes of long duration (none longer than 1 s) or of very wide range extent in the radar data. The two storms on 20 June that exhibited cyclical changes of the propagation effect were characterized by lightning echoes that were infrequent but of very long duration; several persisted for 0.9–1.2 s.

Low reflectivity and small size of storms prevented the detailed analysis of propagation effects in some cases and may have resulted in the obscuration of these effects in other cases. However, from our data, we cannot determine whether this is simply a matter of signal-to-noise ratio or is fundamentally related to storm intensity. For example, at the elevation angle of maximum propagation effect in the first observation of storm A on 8 June, the signal-to-noise ratio exceeded 5 dB in a range interval of about 20 km (34 gates) and exceeded 10 dB in 3 gates. At the elevation angle of

maximum propagation effect in the first observation of storm B on 8 June the signal-to-noise ratio exceeded 5 dB only intermittently in a range interval of about 10 km (17 gates) at altitudes of 7.9–9.7 km. The most active storms on 20 June and 11 August exhibited reflectivity aloft that was comparable to that of storm A of 8 June. As noted in section 5d, most of the storms we observed on other days were of smaller extent either horizontally or vertically or both. In some of these cases, a closer setting of the range gates might have yielded useful measurements. Optimizing the range gates is part of the problem of observational procedure discussed above.

Our observations were further constrained by our dependence on detecting lightning channels in the radar beam as indicators of changing electric fields. This constraint would be more severe at shorter radar wavelengths because of the differing wavelength dependence of backscatter from hydrometeors and from lightning channels. Krehbiel et al. (1991, 1992, 1994) have used other instrumentation to detect lightning and have only occasionally detected echoes from lightning channels in their radar beam. A. Hendry (1989, personal communication) rarely observed lightning echoes; the relatively short wavelength of their radar (1.8 cm) may have precluded detection of lightning in all but the most tenuous of meteorological backscatter media.

c. *Microphysics*

The observed effects depend on the size, shape, and number concentration of the particles in ways that are not well understood. Nevertheless, our measurements can be used to derive some estimates of cloud physical parameters. Weinheimer and Few (1987) calculated electrical and dynamical forces on ice spheroids and found that electric fields of 10 and 100 kV m^{-1} would orient particles having maximum dimensions up to about 50 μm and 1 mm, respectively. The timescale of the orientation is governed by the dielectric relaxation time, which is 1.3 ms or less at temperatures above −40°C. Therefore, the duration of a lightning event, which is typically a few tenths of a second or longer, effectively determines the timescale of the rapid changes of orientation that are observable in the radar measurements. Vivekanandan et al. (1994) used calculations of forward scattering by ice particles with a gamma size distribution to derive the equation

$$K_{DP} = \frac{47.4}{\lambda}(1 - r)^{1.2}\rho^{-0.033}\text{IWC}, \qquad (4)$$

which relates the specific differential phase shift K_{DP} (° km^{-1}) to the wavelength λ (mm), the axial ratio r, the bulk density ρ (g cm^{-3}), and the ice water content IWC (g m^{-3}). If we use Eq. (4) with a wavelength of 111 mm, bulk density of 0.9 g cm^{-3}, axial ratios of 0.1–0.2, and differential phase shift of 0.5° km^{-1}, we derive an IWC of 1.3–1.5 g m^{-3}. If we approximate the particles by prolate spheroids with a maximum dimension of 0.5–1 mm, we obtain number concentrations of 1×10^4–3×10^5 m^{-3}. These values of ice water content and number concentration appear reasonable in comparison to values that have been measured elsewhere (e.g., Heymsfield and Palmer 1986). One of the cases presented by Heymsfield and Palmer included measurements at 8–9 km in altitude in a thunderstorm. If we apply the relationship they derived between reflectivity and ice water content in that case,

$$Z_e = 15.2 \log_{10}\text{IWC} + 20.7, \qquad (5)$$

we find that reflectivity of 20 dBZ, observed in the region of strong propagation effects in storm A on 8 June 1992, implies ice water content of 0.9 g m^{-3}. The proximity of this estimate of ice water content to that derived from Eq. (4) suggests that all the particles in the upper region of the storm are oriented by the electric field. This result implies that the backscatter term in the CCAR varies with the electric field; however, because of the large propagation effects, the backscatter term is effectively unmeasurable in our observations.

The larger values of specific differential phase shift observed in some storms in smaller intervals of range yield unrealistically large values of ice water content when used in Eq. (4). With the same values of parameters as used above, except with K_{DP} = 1.0° km^{-1}, we obtain IWC = 2.6–3.1 g m^{-3} and, with K_{DP} = 1.5° km^{-1}, we obtain IWC = 4.0–4.6 g m^{-3}. Radar calibration accuracy may be an issue in some of these cases, or these conditions may be in nature, as in our measurements, rare events. A more complete understanding of these relationships will require radar measurements with coordinated documentation of microphysical and electrical characteristics and also theoretical studies involving calculations of signal propagation through ice particles.

7. Conclusions

The most significant conclusion to be drawn from these observations is that the effects of rapidly changing electric fields are discernible not in quantities related to backscatter [the first term in Eq. (2)] but in quantities related to propagation [the second term in Eq. (2)]. This result is contrary to what one might have expected for observations with a radar of our wavelength because the differential attenuation and differential phase shift are both very small, especially for propagation through ice particles.

The observed effects include specific differential phase shifts up to 1.6° km^{-1} in range intervals of a few kilometers and smaller phase shifts in range intervals up to 18 km. These occur at altitudes of 7–11 km in thunderstorms. Because the effects are highly localized in space, they are difficult to observe with a single radar. Observation of the propagation effects would be greatly aided by a second radar to maintain continuous sur-

veillance and by a real-time display of quantities derived from the cross-covariance of the two received signals.

The dominance of propagation effects in our observations and the fact that the propagation quantities increase in magnitude as radar wavelength decreases lead to the hypothesis that the sudden changes of cross correlation (both increases and decreases) coincident with lightning that have been observed by radars of shorter wavelength are *all* primarily due to changes in the propagation medium and only secondarily due to changes in the backscatter medium. This hypothesis, if valid, will be of importance in the design of radars for observation of storm electrical phenomena, both for research and for operational applications. The significance of propagation effects in revealing the electrical characteristics of storms implies that radars of shorter wavelength must play a part in future investigations of storm electrical phenomena. However, the fact that these effects are detectable by a radar with a wavelength of 11 cm suggests that a radar optimized for long-range weather surveillance could, with the necessary polarimetric capability and with appropriate scan strategies, detect electrical attributes of storms.

Acknowledgments. I am grateful to Mr. Timothy Hiett and Master Sergeant Richard Chanley, USAF (Retired), who developed and maintained much of the instrumentation and assisted me in radar operations, and to Mr. Kenneth Glover, Chief of the Ground Based Remote Sensing Branch, who supported this work strongly at every stage. The display of lightning data at the radar field site, which was an essential part of the measurement campaign, was made possible by the combined efforts of Dr. Albert Brown of the Atmospheric Structure Branch, Mr. Frank Ruggiero of the Atmospheric Prediction Branch, and Mr. Charles Ivaldi of Atmospheric and Environmental Research, Inc., working on a contract with the Satellite Meteorology Branch. I also appreciate the assistance of Dr. Alexander Kostinski of Michigan Technological University, who visited the radar field site in June 1992 and participated in the observations of 8 June. Dr. Paul Krehbiel of New Mexico Institute of Mining and Technology provided valuable guidance related to instrumentation, experimental procedures, and analysis. Dr. Jothiram Vivekanandan and Dr. Andrew Heymsfield of the National Center for Atmospheric Research assisted me in the microphysical interpretation of the data. This research was sponsored, in part, by the Air Force Office of Scientific Research.

REFERENCES

Hendry, A., and G. C. McCormick, 1976: Radar observations of the alignment of precipitation particles by electrostatic fields in thunderstorms. *J. Geophys. Res.*, **81,** 5353–5357.

——, and Y. M. M. Antar, 1982: Radar observations of polarization characteristics and lightning-induced realignment of atmospheric ice crystals. *Radio Sci.*, **17,** 1243–1250.

Heymsfield, A. J., and A. G. Palmer, 1986: Relationships for deriving thunderstorm anvil ice mass for CCOPE storm water budget estimates. *J. Climate Appl. Meteor.*, **25,** 691–702.

Krehbiel, P. R., W. Rison, S. McCrary, T. Blackman, and M. Brook, 1991: Dual-polarization radar observations of lightning echoes and precipitation alignment at 3 cm wavelength. Preprints, *25th Int. Conf. Radar Meteor.*, Paris, France, Amer. Meteor. Soc., 901–904.

——, T. Chen, S. McCrary, W. Rison, G. Gray, T. Blackman, and M. Brook, 1992: Lightning precursor signatures from dual-polarization radar measurements of storms. *URSI Commission F Open Symp.*, Ravenscar, U. K., Int. Union of Radio Science.

——, ——, ——, ——, ——, and M. Brook, 1994: The use of dual-polarization radar for remotely sensing storm electrification. *Meteor. and Atmos. Phys.*, in press.

McCormick, G. C., and A. Hendry, 1975: Principles for the radar determination of the polarization properties of precipitation. *Radio Sci.*, **10,** 421–434.

——, and ——, 1976: Polarization-related parameters for rain: Measurements obtained by radar. *Radio Sci.*, **19,** 731–740.

Metcalf, J. I., 1988: Precipitation and lightning measurements by polarization diversity radar. AFGL-TR-88-0215, Air Force Geophysics Laboratory, AD A213810, 20 pp.

——, 1992: Radar observations of the effects of changing electric fields on the orientations of hydrometeors. PL-TR-92-2122, Phillips Laboratory, Air Force Systems Command, AD A256712, 30 pp.

——, A. W. Bishop, R. C. Chanley, T. C. Hiett, and P. J. Petrocchi, 1993: An 11-cm coherent polarimetric radar for meteorological research. *J. Atmos. Oceanic Technol.*, **10,** 249–261.

Orville, R. E., R. W. Henderson, and L. F. Bosart, 1983: An East Coast lightning detection system. *Bull. Amer. Meteor. Soc.*, **64,** 1029–1037.

Rison, W., G. Gray, P. R. Krehbiel, and T. Chen, 1993: A compact real-time radar signal processing and display system. Preprints, *26th Int. Conf. Radar Meteor.*, Norman, OK, Amer. Meteor. Soc., 258–260.

Vivekanandan, J., V. N. Bringi, A. Hagen, and P. Meischner, 1994: Polarimetric radar studies of atmospheric ice particles. *IEEE Trans. Geosci. Remote Sens.*, **32,** 1–10.

Weinheimer, A. J., and A. A. Few, 1987: The electric field alignment of ice particles in thunderstorms. *J. Geophys. Res.*, **92,** 14 833–14 844.

Williams, E. R., S. G. Geotis, and A. B. Bhattacharya, 1989: A radar study of the plasma and geometry of lightning. *J. Atmos. Sci.*, **46,** 1173–1185.